Catalysis Science & Technology

PAPER

View Article Online
View Journal | View Issue

Published on 22 October 2013. Downloaded by Brown University on 28/10/2014 13:38:26.

Cite this: *Catal. Sci. Technol.*, 2014, **4**, 411

Synthesis and characterization of chiral recyclable dimeric copper(II)–salen complexes and their catalytic application in asymmetric nitroaldol (Henry) reaction†

Anjan Das,[ab] Rukhsana I. Kureshy,*[ab] P. S. Subramanian,[ab] Noor-ul H. Khan,[ab] Sayed H. R. Abdi[ab] and Hari C. Bajaj[ab]

Received 27th August 2013,
Accepted 21st October 2013

DOI: 10.1039/c3cy00638g

www.rsc.org/catalysis

Six new chiral tridentate ditopic ligands with ONO donors possessing different linkers (either achiral or chiral) were synthesized. The characterization of these ligands was accomplished by IR, UV/Vis, NMR, mass spectrometry and optical rotation. These ligands have been treated with a series of metal ions *viz.*, Cu(II), Cu(I), Co(III) and Zn(II), affording varieties of new chiral metal complexes, which have been characterized thoroughly using different analytical and spectroscopic methods. All the complexes were screened for catalytic asymmetric nitroaldol reaction using benzaldehyde as a model substrate. The reaction conditions were optimized and 79% yield with good enantioselectivity (88%) was achieved at RT with the *in situ* generated catalyst having a piperazine linker and (1*R*,2*S*)-2-amino-1,2-diphenylethanol collar in combination with cupric acetate as the metal source. By applying other aromatic and aliphatic aldehydes, similar yields of β-nitroalcohols with improved enantioselectivities (up to 93%) were achieved. The catalytic system worked very well for up to four cycles with retention of activity and enantioselectivity of β-nitroalcohols.

Introduction

The asymmetric nitroaldol reaction is a powerful and economically viable tool for the synthesis of β-nitroalcohols.[1] Asymmetric nitroaldol reaction generally requires the use of a chiral transition metal complex derived from Co(II),[2] Mg(II),[3] Zn(II),[4] Cr(III),[5] Cu(II),[6] rare earth metals[7] or organocatalysts[8] in order to get high product yield and enantioselectivity. Chronologically, Shibasaki and coworkers[7a–c] demonstrated the first bifunctional lanthanum–lithium chiral binaphthoxide complex as an efficient catalyst for the asymmetric nitroaldol reaction. This was followed by Trost *et al.*'s novel family of dinuclear zinc complexes.[4a,b] Over the period various chiral ligands like BOX[9] and salen-type C_2-symmetric ligands[10] have hogged the limelight as "privileged chiral ligands" in the enantioselective nitroaldol reaction. However, most of these complexes have shown good to excellent enantioselectivities for the nitroaldol reaction at very low temperatures and at high catalysts loading. Therefore, further work is required to address these issues and also the issue of catalyst recyclability in order to ease the high cost of chiral catalysts, thereby making this strategy industrially more acceptable. Recently, we have reported the chiral macrocyclic salen and [H_4]salen complexes of copper(II) salts as very efficient catalysts for the asymmetric nitroaldol reaction of aldehydes with nitromethane to give excellent enantioselectivity and diastereoselectivity.[11] In line with our continued interest in developing recyclable catalysts, here we have synthesized a series of new chiral recyclable tridentate ONO donor dimeric ligands derived from different achiral and chiral linkers *viz.*, piperizine, homopiperazine, trigol, (*R*)- and (*S*)-binol with (1*R*,2*S*)-2-amino-1,2-diphenylethanol and their respective complexes with Cu(II). At first these complexes were generated *in situ* with the aim of evaluating the influence exerted by each ligand on the catalytic activity and enantioselectivity of the nitroaldol product. The best ligand, which is $\mathbf{L^2}$ in the present case, was then complexed *in situ* with several other metal ions *viz.*, Cu(I), Co(III) and Zn(II) to find the most suitable metal complex for the asymmetric nitroaldol reaction. To further refine the results and understand the structure of the active catalyst, Cu(II) complexes of ligands $\mathbf{L^1}$–$\mathbf{L^6}$ were synthesized and characterized by CD, magnetic moment and EPR

[a] *Discipline of Inorganic Materials and Catalysis, Central Salt and Marine Chemicals Research Institute (CSIR-CSMCRI), Bhavnagar, 364 002, India. E-mail: rukhsana93@yahoo.co.in; Fax: +91 0278 2566970*

[b] *Academy of Scientific and Innovative Research (AcSIR), CSIR-CSMCRI, Bhavnagar, Gujarat 364021, India*

† Electronic supplementary information (ESI) available: ^{1}H-NMR data, optical rotation value and HPLC profiles of nitroaldol product. See DOI: 10.1039/c3cy00638g

Published on 22 October 2013. Downloaded by Brown University on 28/10/2014 13:38:26.

investigations. Among these, the complex originating from L^2 with copper(II) acetate was found to be the best catalyst to give the nitroaldol product in high yield and ee up to 93%, and is explored in detail in the present manuscript.

Results and discussion

Chiral ligands L^1–L^6 were synthesized conveniently by the reaction of (1*R*,2*S*)-2-amino-1,2-diphenylethanol with different bis-aldehydes in high yield according to Scheme 1.

The ligands L^1–L^4 possess metal binding chiral domains at terminal coordinating sites with achiral linkers, whereas L^5 and L^6, are composed with chiral motifs both in the terminal and linker regions. ^{1}H-NMR shows only one singlet observed at 1.26–1.60 and 7.81–8.00 ppm for *t*-Bu protons and azomethine proton, respectively, and the MS spectra confirming the dimeric structure together support the formation of C_2 symmetry of salen ligands L^1–L^6. Similarly, the phenolic –OH proton also appeared as singlet for L^1–L^6 at 13.46–13.67 ppm, confirming the dimeric C_2 symmetric structure for all the ligands. After the successful synthesis and characterization of dimeric ligands L^1–L^6, first we screened the ligands (10 mol%) with cupric acetate as metal source in the asymmetric nitroaldol reaction of benzaldehyde as a model substrate with nitromethane in dichloromethane at RT for 30 h and the results are depicted in Table 1. In the first set of screening *in situ* generated complexes derived from the ligands L^1–L^4, we altered the achiral linker (methylene, piperizine, homopiperazine and trigol) at 5,5′-positions of the salen unit by fixing the aminoalcohol functionality originating from (1*R*,2*S*)-2-amino-1,2-diphenylethanol. Among all the ligands used, ligands L^1 and L^2 were found to be more active than the rest. However, L^2 was found to the best both in terms of yield and enantioselectivity (Table 1, entry 2). The consideration of ligands L^5 and L^6 for this reaction was based on our past experience that an additional element of chirality originating from (*R*)-binol/(*S*)-binol in the catalytic concoction improves the enantioselectivity remarkably.[12] But, in the present case the presence of additional chirality was counterproductive and the ligand L^2 was still the best (Table 1, entry 2).

Having identified the L^2 for its superior catalytic activity, the ligand L^2 was allowed to react with several other metal source, such as $ZnEt_2$, $Co(OAc)_2$, CuBr and $CuCl_2{\cdot}2H_2O$ to generate the active catalyst in order to look for the possibility of further improving the yield and enantioselectivity of the

Table 1 Screening of ligands for the asymmetric nitroaldol reaction[a]

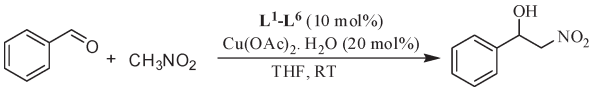

Entry	Ligand	Yield[b] (%)	ee[c] (%)
1	L^1	55	45(*S*)
2	L^2	67	70(*R*)
3	L^3	60	40(*R*)
4	L^4	45	36(*R*)
5	L^5	35	12(*R*)
6	L^6	30	25(*R*)

[a] All the reactions were carried out on a scale of 0.5 mmol of the aldehyde. [b] Isolated after column flash chromatography. [c] Determined by HPLC using chiral column OD.

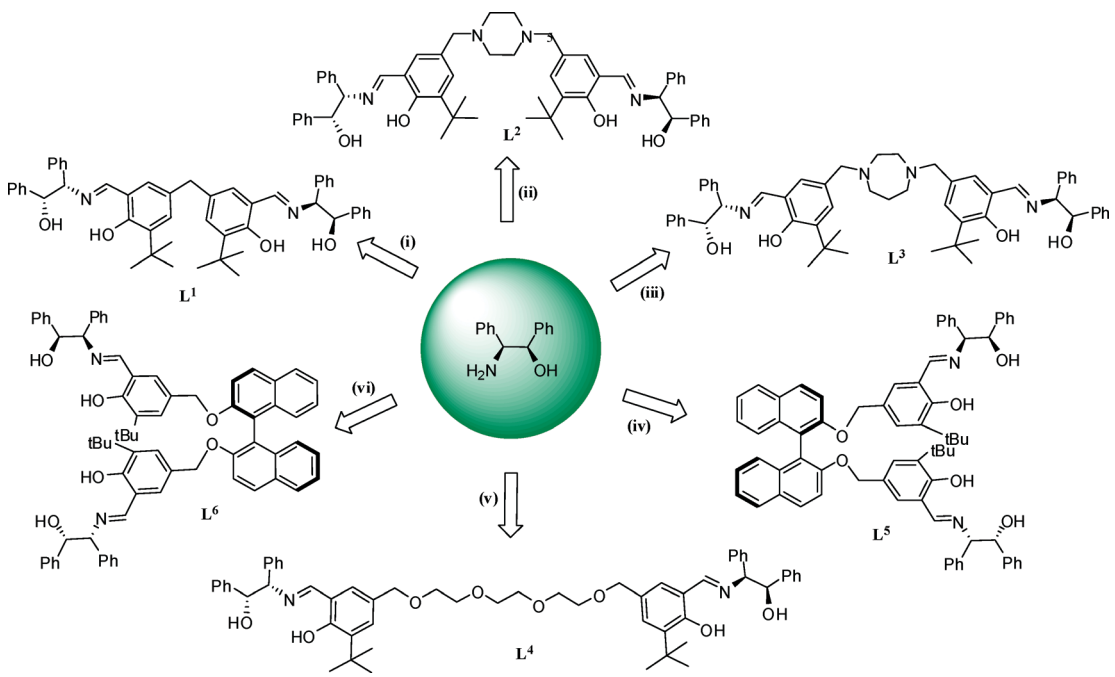

Scheme 1 Synthesis of chiral ligands with (1*R*,2*S*)-2-amino-1,2-diphenylethanol with various bis-aldehydes. (i) Bis-aldehyde, (1*R*,2*S*)-2-amino-1,2-diphenylethanol, dry MeOH, RT. (ii) Piperazine bis-aldehyde, (1*R*,2*S*)-2-amino-1,2-diphenylethanol, dry MeOH, RT. (iii) Homo-piperazine bis-aldehyde, (1*R*,2*S*)-2-amino-1,2-diphenylethanol, dry MeOH, RT. (iv) (*R*)-Binol, (1*R*,2*S*)-2-amino-1,2-diphenylethanol, dry DCM + MeOH, RT. (v) Trigol bis-aldehyde, (1*R*,2*S*)-2-amino-1,2-diphenylethanol, dry MeOH, RT. (vi) (*S*)-Binol, (1*R*,2*S*)-2-amino-1,2-diphenylethanol, dry DCM + MeOH, RT.

 This journal is © The Royal Society of Chemistry 2014

Published on 22 October 2013. Downloaded by Brown University on 28/10/2014 13:38:26.

β-nitroalcohol (Table 2). The results clearly show the suitability of copper metal precursors $Cu(OAc)_2{\cdot}H_2O$, $CuCl_2{\cdot}2H_2O$ and CuBr over $ZnEt_2$ and $Co(OAc)_2$ where poor enantioselectivities (<5% ee) were obtained with moderate to good yield. Among the copper sources used, $Cu(OAc)_2{\cdot}H_2O$ in combination with the ligand $\mathbf{L^2}$ gave the best catalytic performance and hence was used for the further optimization of reaction conditions.

Solvent is known to greatly influence the catalytic performance of the nitroaldol reaction. Accordingly, different solvents like CH_2Cl_2, $CHCl_3$, CH_3CN, CH_3OH and THF (Table 3, entry 1–5) were screened at RT, where THF was found to be best for getting higher ee (84%, entry 5). Next, the catalyst loading variation from 2–15 mol% (Table 3, entries 6–8) suggests 5 mol% loading is optimum at RT, which remained optimum (entry 7) over the temperature range studied from −10° C–RT (Table 3, entry 9–12). The data in Table 3 revealed that 5 mol% ligand in THF as solvent at RT are the optimum reaction parameters to get best catalytic activity and enantioselectivity (Table 3, Entry 7).

After achievement of promising results from benzaldehyde under the optimized reaction conditions, a series of aldehydes (both aromatic and aliphatic) were screened (Table 4). In general, substrates irrespective of electron donating or withdrawing group on the phenyl ring attached to the aldehyde functional group gave products with very good to excellent ee in 30 h. This catalytic protocol also worked well with aliphatic aldehydes *viz.*, *n*-hexanal and cyclohexanal.

It has been observed that among all the combinations of ligand and metal, the ligand $\mathbf{L^2}$ and cupric acetate was identified as the best catalytic system. Nevertheless, all the complexes $\mathbf{C^1}$–$\mathbf{C^6}$ incorporating the ligands $\mathbf{L^1}$–$\mathbf{L^6}$ and cupric acetate were prepared and characterized by different techniques, such as IR, UV-visible spectroscopy, CD and EPR spectral study.

The IR spectra for all the ligands show a characteristic stretching band attributable to νC=N in the range of 1620–1632 cm^{-1} is found shifted to 10–15 cm^{-1} to lower wave number in their respective metal complexes indicating their coordination with Cu(II) metal centre. All these complexes were characterized using positive ion MS spectra. Ligands $\mathbf{L^1}$–$\mathbf{L^6}$ behave very similarly and depict a characteristic ionization peak with one hydrogen ion adduct, while the respective binuclear complexes are obtained with one or two sodium ion adducts; such observation is a well known phenomenon in LC-mass spectrometry.[13]

All the binuclear Cu(II) complexes are soluble in THF. The electronic spectrum for the ligands $\mathbf{L^1}$–$\mathbf{L^6}$ and their complexes with cupric acetate in THF are quite similar. Fig. 1 represents the UV-vis spectra recorded for complexes $\mathbf{C^2}$, $\mathbf{C^4}$, $\mathbf{C^5}$ and $\mathbf{C^6}$ embedded with their respective ligand spectra. All these ligands show a symmetrical narrow band at 340 nm found to be red shifted to 400 nm in the respective Cu(II) complexes, which may be assigned to the ligand to metal

Table 2 Screening of metal salts for the asymmetric nitroaldol reaction[a]

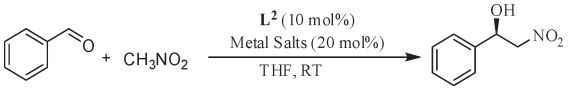

Entry	Ligand	Metal source	Yield[b] (%)	ee[c] (%)
1	$\mathbf{L^2}$	$Cu(OAc)_2{\cdot}H_2O$	67	70
2	$\mathbf{L^2}$	$ZnEt_2$	82	3
3	$\mathbf{L^2}$	$Co(OAc)_2$	54	5
4	$\mathbf{L^2}$	CuBr	56	65
5	$\mathbf{L^2}$	$CuCl_2{\cdot}2H_2O$	45	54

[a] All the reactions were carried out with 0.5 mmol scale of the aldehyde. [b] Isolated after column flash chromatography. [c] Determined by HPLC using chiral column OD.

Table 3 Optimization of asymmetric nitroaldol reaction of various aldehydes with nitromethane[a]

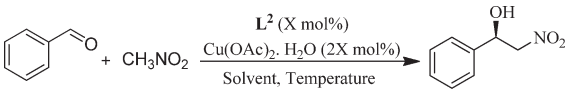

Entry	Ligand (mol%)	Solvents	Temp. (°C)	Yield[b] (%)	ee[c] (%)
1	(10)	CH_2Cl_2	RT	67	70
2	(10)	MeOH	RT	56	56
3	(10)	CH_3CN	RT	57	67
4	(10)	$CHCl_3$	RT	60	68
5	(10)	THF	RT	70	84
6	(2)	THF	RT	65	80
7	(5)	THF	RT	78	88
8	(15)	THF	RT	79	86
9	(5)	THF	0	60	87
10	(5)	THF	−5	50	88
11	(10)	THF	−10	50	89
12	(10)	THF	10	65	86

[a] All the reactions were carried out with 0.5 mmol scale of the benzaldehyde. [b] Isolated after column flash chromatography. [c] Determined by HPLC using chiral column OD, AD, OD-H, AD-H.

Table 4 Variation of different substrates under the optimized reaction conditions[a]

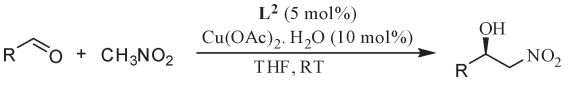

Entry	R	Yield[b] (%)	ee[c] (%)
1	C_6H_5	78	88
2	2-F–C_6H_5	67	78
3	4-F–C_6H_5	70	85
4	2-Cl–C_6H_5	70	90
5	2-MeO–C_6H_5	68	93
6	3-MeO–C_6H_5	72	90
7	4-MeO–C_6H_5	75	89
8	3-NO_2–C_6H_5	80	75
9	4-NO_2–C_6H_5	82	78
10	2-Br–C_6H_5	64	88
11	4-Br–C_6H_5	65	89
12	*n*-Hexanal	67	90
13	Cyclohexanal	68	91
14	4-OH–C_6H_5	62	82
15	4-CH_3CONH–C_6H_5	70	86

[a] All the reactions were carried out with 0.5 mmol scale of the aldehyde. [b] Isolated after column flash chromatography. [c] Determined by HPLC using chiral column OD, OD-H, AD, AD-H, IC.

Published on 22 October 2013. Downloaded by Brown University on 28/10/2014 13:38:26.

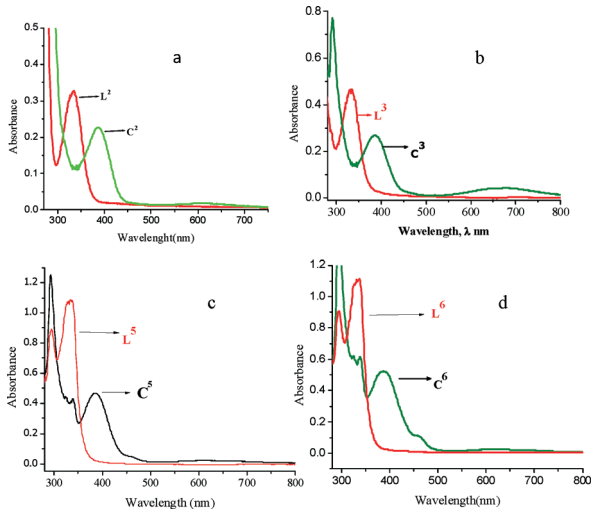

Fig. 1 UV–visible spectra of 0.1 M solution of ligand using THF at RT: (a) L^2 and C^2; (b) L^3 & C^3; (c) L^5 & C^5; (d) L^6& C^6.

charge transfer of non-bonding lone pair of the phenolate oxygen to the d-orbitals of the Cu(II), *i.e.*, LMCT and affirms the formation of complexes of the ligands with cupric acetate. The broad spectral feature centred at 630 nm in the visible region obtained for almost all the complexes may be attributed to the d–d transition. The position of the d–d band supports the tetrahedrally distorted square planar geometry around Cu(II) centres.

The complexes C^1–C^4 possess similar chiral components, while the complexes C^5 and C^6 differ and possess an additional chiral spacer, binol. Binol is known for its axial chirality. Hence systematic circular dichroism (CD) spectral investigation was carried out for the ligands and their respective complexes and are presented in Fig. 2. The CD pattern for ligand L^1 and L^2 are similar, while their respective metal complexes C^1 and C^2 are opposite to each other. This may be due to opposite stereochemical arrangements with respect to their ligands, which make the metal centre chiral and cause their metal centered d–d transitions with negative and positive Cotton effects. Generally chirality at the metal center might result in "Δ" or "Λ" based on their stereochemical chromophoric arrangements.[14] Since complexes C^1–C^6 are binuclear in nature the possible combination for the "chirality at metal" would be $\Delta\Delta$, $\Delta\Lambda$ or $\Lambda\Lambda$. The CD pattern obtained for C^1 and C^2 clearly show negative and positive Cotton effects in their respective d–d transitions. Hence it is obvious to assume that these complexes possess predominantly $\Delta\Delta$ or $\Lambda\Lambda$ and governs the configuration of the nitroaldol product (Table 1, entries 1, 2). But in the cases of C^3 and C^4, the respective CD patterns attributable to d–d band being almost flat, the spectra show that these complexes possess equivalent mixture of both conformational isomers $\Delta\Lambda$ or $\Delta\Delta \approx \Lambda\Lambda$, which might have cancelled each other. With the metal centered chirality thus being a key factor for any catalytic reaction, the observation from Table 1 supports that C^1 and C^2 due to their dominance in $\Delta\Delta$ or $\Lambda\Lambda$ show higher enantioselectivity in the nitroaldol product, while C^3 and C^4 are less enantioselective, due to the presence of both geometrical isomers *i.e.*, $\Delta\Lambda$ or $\Delta\Delta \approx \Lambda\Lambda$.

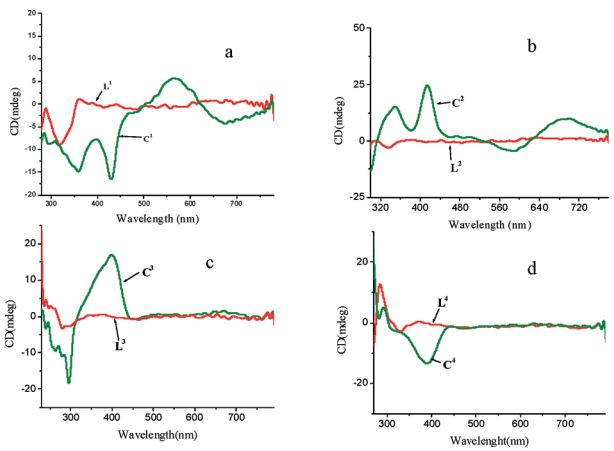

Fig. 2 CD spectra for (a) L^1 and C^1, (b) L^2 and C^2, (c) L^3 and C^3, (d) L^4 and C^4 recorded in THF. Conc. 1×10^{-4} M.

Magnetic moment studies

The ligand being ditopic, all six complexes are composed of two copper(II) ions and hence to understand intermetallic magnetic interactions, and their impact on the catalytic efficiency, we have determined the magnetic moment using Evans' method in solution state.[15] Accordingly, the magnetic moments for C^1–C^6 were obtained in the range 1.72 to 1.78 BM per Cu(II) ion, falling well within the range reported for monomeric species,[16] indicate that in the dimeric structure, all Cu(II) ions are well separated from each other and are non-interacting. This observation suggests that the intermetallic linkers in the dimeric system are not favouring the M–M exchange interaction.

In addition to the magnetic moment measurement further confirmation was established using solution state EPR spectra. Since the complex C^2 gave higher catalytic yield and enantioselectivity, we were encouraged to investigate the geometry of the Cu(II) centres in the bimetallic system. Accordingly, the EPR spectrum for complex C^2 was recorded using liquid nitrogen at 77 K in THF and is depicted in Fig. 3. A typical four line hyperfine feature corresponding to the interaction of the unpaired electron (^{63}Cu and ^{65}Cu) with the

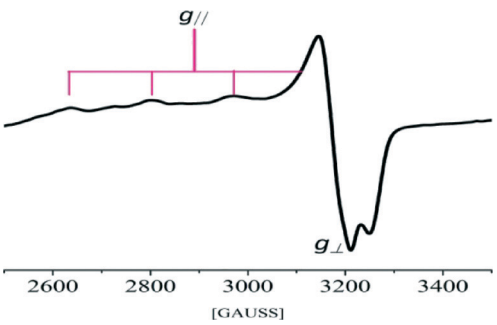

Fig. 3 X-band EPR spectrum recorded for complex C^2 in THF solvent, frozen at 77 K with liquid nitrogen.

This journal is © The Royal Society of Chemistry 2014

Published on 22 October 2013. Downloaded by Brown University on 28/10/2014 13:38:26.

nuclear spin $I = 3/2$ attributable to −3/2, −1/2, +1/2, +3/2 transitions ($\delta = \pm 1$) is generally observed for monomeric species. Similarly a weak signal attributable to $\Delta Ms = \pm 2$ transition in the half field region is the characteristic peak generally observed for dinuclear Cu(II) system. The absence of the $\Delta Ms = \pm 2$ transition in the present case thus rules out the possibility of any Cu–Cu dimeric exchange interactions in the binuclear system although the complex is binuclear in nature. Further, the Cu(II) d^9 system in complex C^2 illustrates characteristic four line peaks as shown in Fig. 3, which is attributable to monomeric species. In the present case, among the four lines observed three are resolved and the fourth line is merged with perpendicular feature. The EPR parameters $g_{\|} = 2.2160$, $A_{\|} = 148$ G, $g_{\perp} = 2.0042$ derived from the spectra suggest that the geometry at the Cu(II) centre might be a tetrahedrally distorted square planar geometry, which is very much in parallel with the d–d band observed in the UV-vis spectra. The position of the EPR signal and the absence of $\Delta Ms = \pm 2$ resonance strongly suggested that the molecule, although binuclear in nature, still possesses a non-interacting M–M association. This observation supporting the monomeric behaviour matches well with the magnetic moment determined above.

Since both the active sites in the catalytic system worked separately for producing enantioselectivity as well as activity, for the evaluation of a probable mechanism of the catalytic nitroaldol reaction, a single unit was considered, which has been shown in Scheme 2. Based on the EPR results a tetrahedrally distorted square planar geometry complex structure was considered for the prediction of the probable mechanism. The aldehyde was coordinated to the vacant d orbital of the copper through the lone pair of the oxygen forming a penta-coordinate transition state (T_1), thereby increasing the electrophilicity of the carbonyl group. The coordination number of the copper centre may be extended to six from five upon further addition of an active nucleophile, nitronate ion, forming a transition state (T_2), where the nitronate ion attacks the activated aldehyde to give the nitroaldol product.

To investigate the reason behind the preferential formation of the *R*-nitroaldol product, a probable transition state involving complex C^2, 2-MeO-benzaldehyde and nitromethane was generated and energy minimized by using ChemDraw 12.0(3D) (Scheme 3). From the TS it is clear that the nitronate ion attacks the carbonyl group of the aldehyde from the Si face, favouring the *R* product.

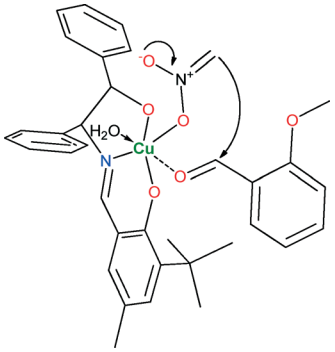

Scheme 3 Energy minimized probable transition state favouring the formation of (*R*)-β-nitroalcohol.

In order to find out the dependence of both yield and enantioselectivity on time, a model reaction of benzaldehyde with nitromethane was carried with the optimal nitroaldol reaction parameters and both the yield and enantioselectivity were plotted against time (Fig. 4). From Fig. 4 it is clear that initially up to 6 h there was a rapid increase in the yield (up to 60%) with slight variation in enantioselectivity. On further increasing the reaction time up to 30 h, there was very slow increase of the yield observed with almost constant enantioselectivity.

Recyclability study of the complex C^2

After the completion of the nitroaldol reaction of the benzaldehyde with nitromethane, the solvent was completely evaporated under reduced pressure and was dried. The product and unreacted substrate were extracted by using non-polar solvent (hexane). Then the isolated catalyst was washed four times with hexane and was dried for 3–4 h under vacuum. The recovered catalyst was used straightaway (without further addition of the metal salt or ligand) for subsequent catalytic cycles. In the case of polar substrates (Table 4, entries 14, 15), the catalysts were separated from the reaction mixtures by passing through a silica pad using EtOAc : hexane (1 : 1) as solvent. The performance of the catalyst remained stable over five catalytic cycles (Fig. 5). From the recycling experiments it is evident that the complex C^2 is stable during the course of the asymmetric nitroaldol reaction, confirmed by the IR spectra (Fig. 6) which matched well with virgin catalyst C^2, suggesting

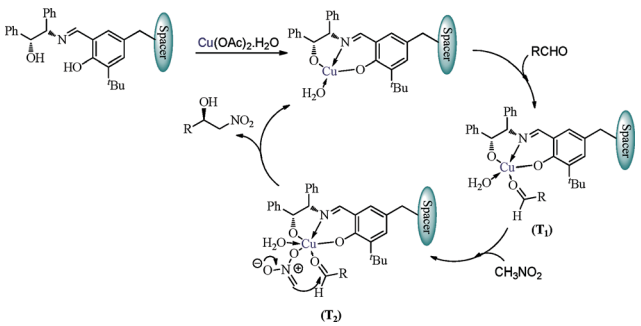

Scheme 2 A probable mechanism for the catalytic asymmetric nitroaldol reaction.

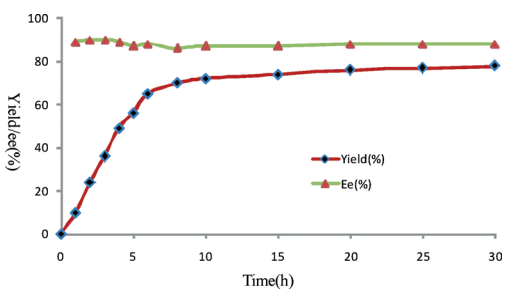

Fig. 4 Variation of yield and ee *vs.* time of nitroaldol reaction of benzaldehyde with nitromethane.

Published on 22 October 2013. Downloaded by Brown University on 28/10/2014 13:38:26.

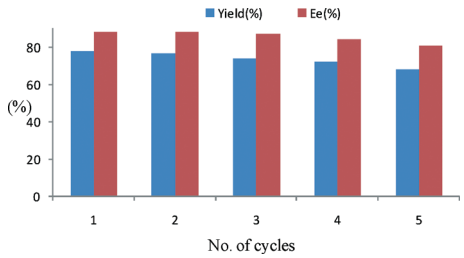

Fig. 5 Recyclability study of the catalytic system using benzaldehyde and nitromethane as model substrates.

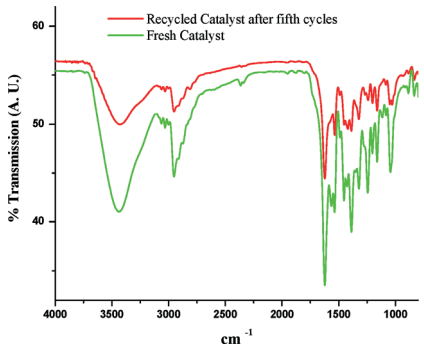

Fig. 6 IR spectra of fresh and recycled catalyst.

that no major structural changes had taken place during the course of post-catalytic workup procedure.

Conclusions

Six chiral ditopic ligands and their respective bimetallic Cu(II) complexes were synthesised and characterized. All these ligands were screened for their catalytic activity in asymmetric nitroaldol reaction. The ligand $\mathbf{L^2}$ in combination with cupric acetate was found to be the catalytically most suitable, and was chosen for further fine tuning of the catalytic studies to obtain the best results. Although we have tested various metals, cupric acetate generates the most active catalytic system with ligand $\mathbf{L^2}$, giving high yield and enantiomeric excess. The CD spectra indicates that the complexes $\mathbf{C^1}$ and $\mathbf{C^2}$ gain metal centred chirality and are dominated by $\Delta\Delta > \Lambda\Lambda$ or $\Delta\Delta < \Lambda\Lambda$, leading to asymmetrically enhanced catalysis. However the other complexes show flat CD patterns with respect to d–d transitions, indicating the existence of a $\Delta\Delta \approx \Lambda\Lambda$ situation. The magnetic properties and the EPR spectra together support the existence of non-interacting Cu–Cu dimers in the case of complex $\mathbf{C^2}$.

Experimental section

General

All the chemicals were purchased from Aldrich & Co. IR spectra were recorded using KBr pellets (1% w/w) on a Perkin-Elmer Spectrum GX FT-IR spectrophotometer. Electronic spectra were recorded on a Shimadzu UV 3101PC spectrophotometer. Mass analyses were performed using positive electron spray ionization (ESI+) technique on a Waters Q Tof-micro mass spectrometer for all these complexes upon dissolving in CH_3CN solvent. ^1H and ^{13}C spectra were recorded on a Bruker Avance II 500 MHz FT-NMR spectrometer. Chemical shifts for proton resonances are reported in ppm (δ) relative to tetramethylsilane. Electron spin resonance spectra were recorded using Bruker X-band electron paramagnetic resonance spectrometer and the DPPH was used as filed marker in the EPR spectra. The CD spectra were recorded on a JASCO 815 Spectrometer. The formation of nitroaldol was determined by HPLC (Shimadzu SCL-10AVP) using Chiracel columns (AD, OD, OD-H).

Typical procedure for the synthesis of ligand $\mathbf{L^1}$–$\mathbf{L^6}$

Various dialdehydes namely, (*S*)-5,5′-(1,1′-binaphthyl-2,2'-diylbis(oxy))bis(methylene)bis(3-*tert*-butyl-2-hydroxybenzaldehyde)/(*R*)-5,5′-(1,1′-binaphthyl-2,2′-diylbis(oxy))bis(methylene)bis(3-*tert*-butyl-2-hydroxybenzaldehyde), 5,5′-(piperazine-1,4-diylbis(methylene))bis(3-*tert*-butyl-2-hydroxybenzaldehyde) and trigol bis-aldehydes were synthesized by the reported procedures[12] and were taken (1 mmol) in 5 ml THF. The solutions were added to a solution of (1*R*,2*S*)-2-amino-1,2-diphenylethanol (2 mmol) and the resulting mass was stirred for 5 h at room temperature (checked by TLC). After the completion of the reaction, the solvent was completely removed under reduced pressure on a rotary evaporator to give chiral salen ligands $\mathbf{L^1}$–$\mathbf{L^6}$ in high yield.

Characterization data of ligands $\mathbf{L^1}$–$\mathbf{L^6}$

$\mathbf{L^1}$. Yellow solid; yield 95%; $[\alpha]_D^{20}$ = −15.44 (c 1, $CHCl_3$); ^1H NMR ($CDCl_3$, 500 MHz, TMS): δ = 13.47 (br. s, 2H), 8.00 (s, 2H), 7.10–7.37 (m, 24H), 6.61 (s, 2H), 5.04 (d, J = 5 Hz, 2H), 4.44 (d, J = 5 Hz, 2H), 3.72 (s, 2H), 1.60 (s, 18H);^{13}C NMR (125 MHz, $CDCl_3$): δ = 29.3, 34.8, 40.2, 78.36, 80.22, 127.2, 127.9, 128.0, 128.1, 129.9, 130.1, 130.5, 137.2, 139.4, 140.1, 158.5, 166.6 ppm. IR (KBr) ν: 3428, 3060, 3030, 3000, 2954, 2908, 2873, 2707, 1955, 1882, 1806, 1753, 1627, 1442 cm^{-1}. Anal. calcd. for $C_{51}H_{54}N_2O_4C$, 80.71; H, 7.17; N, 3.69; found: C, 80.68; H, 7.19; N, 3.68. LC-MS: m/z 759 $[M + H]^+$.

$\mathbf{L^2}$. Yellow solid; yield 85%; $[\alpha]_D^{20}$ = −25.54 (c 1, $CHCl_3$); ^1H NMR ($CDCl_3$, 200 MHz, TMS): 13.52 (s, 2H), 8.07 (s, 2H), 7.36–7.15 (m, 24H), 5.06, 5.03 (d, J = 7 Hz, 2H), 4.49–4.46 (d, J = 7 Hz, 2H), 3.35 (s, 4H), 2.37 (s, 8H) 1.41 (s, 18H); ^{13}C NMR (125 MHz, $CDCl_3$) 166.32, 158.60, 139.12, 138.32, 136.22, 130.65, 130.51, 127.50, 126.90, 126.76, 126.22, 117.22, 79.85, 78.10, 60.62, 52.42, 34.72. IR (KBr) ν: 3426, 3062, 3030, 2952, 2875, 2812, 1884, 1808, 1628, 1447, 1384 cm^{-1}. Anal. calcd. for $C_{56}H_{64}N_4O_4$ C, 78.47; H, 7.53; N, 6.54; found: C, 78.45; H, 7.52; N, 6.55. LC-MS: m/z 857 $[M + H]^+$.

$\mathbf{L^3}$. Yellow solid; yield 85%; $[\alpha]_D^{20}$ = −12.56 (c 1, $CHCl_3$), ^1H NMR ($CDCl_3$, 200 MHz, TMS): δ ppm = 13.67 (s, 2H), 8.08 (s, 2H), 7.32–7.19 (m, 24H), 5.01–5.00 (d, J = 2 Hz, 2H), 5.49–5.48 (d, J = 2 Hz, 2H), 3.53 (s, 4H), 2.70–2.63 (m, 8H), 1.79 (s, 2H), 1.49 (s, 18H); ^{13}C NMR (125 MHz, $CDCl_3$)

 This journal is © The Royal Society of Chemistry 2014

Published on 22 October 2013. Downloaded by Brown University on 28/10/2014 13:38:26.

166.37, 159.62, 140.13, 139.36, 137.20, 130.68, 130.56, 128.51, 127.99, 127.79, 127.20, 118.23, 79.89, 78.16, 61.65, 53.43, 34.74, 29.27. IR (KBr) *v*: 3370, 3062, 3030, 2952, 2916, 2871, 2246, 1954, 1881, 1807, 1745, 1629, 1447, 1388 cm^{-1}. Anal. calcd. for $C_{57}H_{66}N_4O_4$ C, 78.59; H, 7.64; N, 6.43; found: C, 78.56; H, 7.65; N, 6.45. LC-MS: *m*/*z* 872 $[M + H]^+$.

L^4. Yellow solid; yield 90%; $[\alpha]_D^{20}$ = −5.42 (c 1, $CHCl_3$); ^1H NMR ($CDCl_3$, 200 MHz, TMS): δ ppm = 13.65 (s, 2H), 8.06 (s, 2H), 7.35–7.22 (m, 24H), 5.04–5.01(d, *J* = 6 Hz, 2H), 4.48–4.45 (d, *J* = 6 Hz, 2H), 4.39 (s, 4H), 3.61–3.57 (m, 12H), 1.42 (s, 18H); ^{13}C NMR (125 MHz, $CDCl_3$) 166.48, 159.58, 140.13, 139.43, 137.34, 129.86, 129.26, 129.15, 128.69, 128.07, 127.55, 127.22, 118.26, 80.19, 73.17, 70.62, 69.13, 34.86, 29.31. IR (KBr) *v*: 3440, 2921, 1632, 1539, 1455, 1385 cm^{-1}. Anal. calcd. for $C_{58}H_{68}N_2O_8C$, 75.62; H, 7.44; N, 3.04; found: C, 75.64; H, 7.42; N, 3.02. LC-MS: *m*/*z* 921 $[M + H]^+$.

L^5. Yellow solid; yield 90%; $[\alpha]_D^{20}$ = −17.24 (c 1, $CHCl_3$), ^1H NMR ($CDCl_3$, 200 MHz, TMS): δ = 13.46 (s, 2H), 7.81 (d, *J* = 9 Hz, 2H), 7.73 (d, *J* = 8 Hz, 2H), 7.58 (s, 2H), 7.36 (m, 8H), 7.31(s, 2H), 7.15–7.25 (m, 14H), 7.05–7.07 (m, 4H), 6.88 (s, 2H), 6.20 (s, 2H), 5.00 (d, *J* = 7 Hz, 2H), 4.80 (s, 4H), 4.38 (d, *J* = 7 Hz, 2H), 1.26 (s, 18H). ^{13}CNMR (50 MHz, $CDCl_3$): 30.30, 30.69, 72.64, 117.86, 122.83, 125.78, 127.13, 128.28, 129.47, 129.65, 131.17, 131.31, 132.11, 134.37, 135.74, 139.49, 162.03. IR (KBr) *v*: 3431, 3059, 3031, 2954, 2921, 2868, 1950, 1805, 1627, 1592, 1502, 1452 cm^{-1}. Anal. calcd. for $C_{72}H_{68}N_2O_6C$, 81.79; H, 6.48; N, 2.65; found: C, 81.76; H, 6.46; N, 2.68. LC-MS: *m*/*z* 1058 $[M + H]^+$.

L^6. Yellow solid; yield 90%; $[\alpha]_D^{20}$ = −27.12 (c 1, $CHCl_3$), ^1H NMR ($CDCl_3$, 200 MHz, TMS): δ = 13.45 (s, 2H), 7.80 (d, *J* = 9 Hz, 2H), 7.72 (d, *J* = 8 Hz 2H), 7.57 (s, 2H), 7.35 (m, 8H), 7.30(s, 2H), 7.14–7.24 (m, 14H), 7.04–7.06 (m, 4H), 6.87 (s, 2H), 6.20 (s, 2H), 5.01 (d, *J* = 7 Hz, 2H), 4.81 (s, 4H), 4.37 (d, *J* = 7 Hz, 2H), 1.25(s, 18H). ^{13}C NMR (50 MHz, $CDCl_3$): 30.30, 30.68, 72.63, 117.85, 122.82, 125.77, 127.12, 128.27, 129.47, 129.64, 131.16, 131.30, 132.10, 134.37, 135.74, 139.46, 162.03. IR (KBr) *v*: 3431, 3059, 3031, 2954, 2921, 2868, 1950, 1805, 1627, 1592, 1502, 1452 cm^{-1}. Anal. calcd. for $C_{72}H_{68}N_2O_6C$, 81.79; H, 6.48; N, 2.65; found: C, 81.75; H, 6.47; N, 2.64. LC-MS: *m*/*z* 1058 $[M + H]^+$.

Characterization data of metal complexes (C^1–C^6)

C^1: IR (KBr) *v*: 3405, 3061, 3029, 2953, 2908, 2872, 2616, 1952, 1881, 1806, 1707, 1621, 1532, 1491, 1420 cm^{-1}. $[\alpha]_D^{20}$ = −35.42 (c 1, $CHCl_3$). LC-MS: *m*/*z* 881 $[Cu_2L^1 + H]^+$. CD (THF) λ_{max} (nm) ($\Delta\varepsilon$): 360.74 (−14.90), 433.70 (−16.43), 563.98 (+5.53), 675.71(−4.48). UV/Vis (THF): λ_{max} (ε) = 625, 385 nm. Anal. calcd. for ($C_{51}H_{50}N_2O_4$): C, 69.45; H, 5.71; N, 3.18; found: C, 69.15; H, 5.66; N, 3.16.

C^2: IR (KBr) *v*: 3436, 3029, 2927, 2802, 1812, 1620, 1533, 1421 cm^{-1}. $[\alpha]_D^{20}$ = 29.25 (c 1, $CHCl_3$). LC-MS: *m*/*z* 979 $[Cu_2L^2 + H]^+$, LC-MS: *m*/*z* 996 $[Cu_2L^2 + H_2O]^+$. CD (THF) λ_{max} (nm) ($\Delta\varepsilon$): 347.86 (+14.62), 415.66 (+24.30), 590.40 (−4.90), 693.82 (+9.97). UV/Vis (THF): λ_{max} (ε) = 630, 390 nm. Anal. calcd. for ($C_{56}H_{60}N_4O_4$): C, 68.62; H, 6.17; N, 5.72; found: C, 68.56; H, 6.10; N, 5.68.

C^3: IR (KBr) *v*: 3430, 2956, 2924, 2359, 1955, 1890, 1735, 1625, 1569, 1435, 1382 cm^{-1}. $[\alpha]_D^{20}$ = 15.58 (c 1, $CHCl_3$). LC-MS: *m*/*z* 1015 $[Cu_2L^3 + Na]^+$. CD (THF) λ_{max} (nm) ($\Delta\varepsilon$): 294.43(−18.63), 397.92(+16.83). UV/Vis (THF): λ_{max} (ε) = 672.36, 388.22 nm. Anal. calcd. for ($C_{57}H_{62}N_4O_4$): C, 68.86; H, 6.29; N, 5.64; found: C, 68.76; H, 6.21; N, 5.62.

C^4: IR (KBr) *v*: 3433, 3030, 2910, 2863, 1954, 1623, 1566, 1536, 1422, 1388 cm^{-1}. $[\alpha]_D^{20}$ = 26.52 (c 1, $CHCl_3$). LC-MS: *m*/*z* 1065 $[Cu_2L^4+Na]^+$. CD (THF) λ_{max} (nm) ($\Delta\varepsilon$): 290.32(+4.73), 391.51(−13.32). UV/Vis (THF): λ_{max} (ε) = 604.44, 385.63 nm. Anal. calcd. for ($C_{58}H_{64}N_2O_8$): C, 66.71; H, 6.18; N, 2.68; found: C, 66.72; H, 6.12; N, 2.62.

C^5: IR (KBr) *v*: 3433, 3058, 3029, 2949, 2861, 2694, 1948, 1806, 1741, 1619, 1535, 1503, 1454 cm^{-1}. $[\alpha]_D^{20}$ = 32.25 (c 1, $CHCl_3$). LC-MS: *m*/*z* 1224 $[Cu_2L^5 + 2Na]^+$. CD (THF) λ_{max} (nm) ($\Delta\varepsilon$): 327.80 (−0.44), 356.57 (−18.92), 414.12 (−19.64), 691.67 (−4.14). UV/Vis (THF): λ_{max} (ε) = 631.82, 389.15 nm. Anal. calcd. for ($C_{72}H_{64}N_2O_6$): C, 73.26; H, 5.47; N, 2.37; found: C, 73.18; H, 5.45; N, 2.36.

C^6: IR (KBr) *v*: 3432, 3057, 3028, 2948, 2860, 2693, 1947, 1805, 1740, 1618, 1534, 1502, 1453 cm^{-1}. $[\alpha]_D^{20}$ = 12.12 (c 1, $CHCl_3$). CD (THF) λ_{max} (nm) ($\Delta\varepsilon$): 324.74 (−36.06), 326.35 (−25.87), 408.00 (−23.02), 680.68 (−5.30). UV/Vis (THF): λ_{max} (ε) = 630, 389 nm. Anal. calcd. for ($C_{72}H_{64}N_2O_6$): C, 73.26; H, 5.47; N, 2.37; found: C, 73.16; H, 5.42; N, 2.35.

Magnetic moment determination

Magnetic susceptibility measurements were carried out as per the procedure reported by Evans. The inner tube (~2.5 mm i.d.) was filled with the known concentration of sample solution in THF + *tert*-butyl alcohol, while the outer tube was filled with THF + *tert*-butyl alcohol. A paramagnetic shift observed in a TMS resonance line was used to calculate χ_M using eqn (1).

$$\chi_M = 3\Delta f/2\pi v + \chi 0 + \chi 0(d0 - ds)/m \quad (1)$$

where *f* = frequency separation between the TMS lines, *fm* = frequency at which the proton resonance is studied, and *m* = mass of the substance. The magnetic moment was calculated from χ_M using eqn (2).

$$\mu_{eff} = \sqrt{\chi_M T} \quad (2)$$

where *T* stands for temperature in K.

Acknowledgements

Anjan Das and RIK are thankful to DST and CSIR-Indus Magic Project CSC0123 for financial assistance. Anjan Das is thankful to UGC for awarding SRF and to AcSIR for Ph.D registration. Authors are also grateful to Analytical Discipline and Centralized Instrument Facility of CSMCRI for providing instrumental facilities.

Published on 22 October 2013. Downloaded by Brown University on 28/10/2014 13:38:26.

Notes and references

1 (*a*) C. Palomo, M. Oiarbide and A. Laso, *Eur. J. Org. Chem.*, 2007, 2561; (*b*) L. C. R. Henry, *C. R. Hebd. Seances Acad. Sci.*, 1895, **120**, 1265; (*c*) E. J. Corey and F. U. Zhang, *Angew. Chem., Int. Ed.*, 1999, **38**, 1931; (*d*) K. Y. Spangler and C. Wolf, *Org. Lett.*, 2009, **11**, 4724; (*e*) M. Bandini, F. Piccinelli, S. Tommasi, A. Umani-Ronchi and C. Ventrici, *Chem. Commun.*, 2007, 616; (*f*) N. Ono, *The Nitro Group in Organic Synthesis*, Wiley-VCH, New, York, 2001.

2 J. Park, K. Lang, K. A. Abboud and S. Hong, *J. Am. Chem. Soc.*, 2008, **130**, 16484.

3 B. M. Choudary, K. V. S. Ranganath, U. Pal, M. L. Kantam and B. Sreedhar, *J. Am. Chem. Soc.*, 2005, **127**, 13167.

4 (*a*) B. M. Trost and V. S. C. Yeh, *Angew. Chem.*, 2002, **114**, 889; (*b*) B. M. Trost, V. S. C. Yeh, H. Ito and N. Bremeyer, *Org. Lett.*, 2002, **4**, 2621; (*c*) A. Bulut, A. Aslan and Ö. Dogan, *J. Org. Chem.*, 2008, **73**, 7373.

5 R. Kowalczyk, Ł. Sidorowicz and J. Skarzewski, *Tetrahedron: Asymmetry*, 2007, **18**, 2581.

6 (*a*) V. J. Mayani, S. H. R. Abdi, R. I. Kureshy, N. H. Khan, A. Das and H. C. Bajaj, *J. Org. Chem.*, 2010, **75**, 6191; (*b*) A. Noole, K. Lippur, A. Metsala, M. Lopp and T. Kanger, *J. Org. Chem.*, 2010, **75**, 1313; (*c*) M. Steurer and C. Bolm, *J. Org. Chem.*, 2010, **75**, 3301; (*d*) G. Blay, V. Hernández-Olmos and J. R. Pedro, *Chem. Commun.*, 2008, 4840; (*e*) T. Arai, M. Watanabe and A. Yanagisawa, *Org. Lett.*, 2007, **9**, 3595; (*f*) R. Kowalczyk and J. Skarżewski, *Tetrahedron: Asymmetry*, 2009, **20**, 2467; (*g*) N. Sanjeevkumar and M. Periasamy, *Tetrahedron: Asymmetry*, 2009, **20**, 1842; (*h*) S. Jammi, M. A. Ali, S. Sakthivel, L. Rout and T. Punniyamurthy, *Chem.–Asian J.*, 2008, **4**, 314; (*i*) S. Jammi, P. Saha, S. Sanyashi and T. Punniyamurthy, *Tetrahedron*, 2008, **64**, 11724; (*j*) B. Quin, X. Xiao, X. Liu, J. Huang, Y. Wen and X. Feng, *J. Org. Chem.*, 2007, **72**, 9323; (*k*) M. Breuning, D. Hein, M. Steiner, V. H. Gessner and C. Strohmann, *Chem.–Eur. J.*, 2009, **15**, 12764; (*l*) M. Bandini, S. Cabiddu, E. Cadoni, P. Olivelli, R. Sinisi, A. Umani-Ronchi and M. Usai, *Chirality*, 2009, **21**, 239; (*m*) I. Panov, P. Drabina, Z. Padělková, P. Šimůnek and M. Sedlák, *J. Org. Chem.*, 2011, **76**, 4787; (*n*) Y. Zhou, J. Dong, F. Zhang and Y. Gong, *J. Org. Chem.*, 2011, **76**, 588; (*o*) M. Zielińska-Błajet and J. Skarżewski, *Tetrahedron: Asymmetry*, 2009, **20**, 1992; (*p*) R. Boobalan, G.-H. Lee and C. Chena, *Adv. Synth. Catal.*, 2012, **354**, 2511.

7 (*a*) T. Arai, Y. M. A. Yamada, N. Yamamoto, H. Sasai and M. Shibasaki, *Chem.–Eur. J.*, 1996, **2**, 1368; (*b*) M. Shibasaki and N. Yoshikawa, *Chem. Rev.*, 2002, **102**, 2187; (*c*) H. Sasai, S. Watanabe, T. Suzuki and M. Shibasaki, *Org. Synth.*, 2004, **10**, 571; (*d*) T. Purkarthofer, K. Gruber, M. Gruber-Khadjawi, K. Waich, W. Skranc, D. Mink and H. Griengl, *Angew. Chem.*, 2006, **118**, 3532.

8 (*a*) E. J. Corey and F.-Y. Zhang, *Angew. Chem., Int. Ed.*, 1999, **38**, 1931; (*b*) T. Ooi, K. Doda and K. Maruoka, *J. Am. Chem. Soc.*, 2003, **125**, 2054; (*c*) H. Li, B. Wang and L. Deng, *J. Am. Chem. Soc.*, 2006, **128**, 732; (*d*) T. Marcelli, R. N. S. Van der Haas, J. H. Van Maarseveen and H. Hiemstra, *Angew. Chem., Int. Ed.*, 2006, **45**, 929; (*e*) T. Nitabaru, N. Kumagai and M. Shibasaki, *Angew. Chem., Int. Ed.*, 2012, **51**, 1644; (*f*) T. Mandal, S. Samanta and C.-G. Zhao, *Org. Lett.*, 2007, **9**, 943.

9 (*a*) D. A. Evans, D. Seidel, M. Rueping, H. W. Lam, J. T. Shaw and C. W. Downey, *J. Am. Chem. Soc.*, 2003, **125**, 12692; (*b*) D.-M. Du, S.-F. Lu, T. Fang and J. Xu, *J. Org. Chem.*, 2005, **70**, 3712; (*c*) G. Blay, E. Climent, I. Fernández, V. Hernández-Olmos and J. R. Pedro, *Tetrahedron: Asymmetry*, 2006, **17**, 2046; (*d*) S. Liu and C. Wolf, *Org. Lett.*, 2008, **10**, 1831; (*e*) H. Y. Kim and K. Oh, *Org. Lett.*, 2009, **11**, 5682.

10 (*a*) M. Çolak, T. Aral, H. Hoşgören and N. Demirel, *Tetrahedron: Asymmetry*, 2007, **18**, 1129; (*b*) Y. Zhang, L. Xiang, Q. Wang, X.-F. Duan and G. Zi, *Inorg. Chim. Acta*, 2008, **361**, 1246; (*c*) C. Palomo, M. Oiarbide and A. Mielgo, *Angew. Chem., Int. Ed.*, 2004, **43**, 5442; (*d*) T. M. Suzuki, M. Yamamoto, K. Fukumoto, Y. Akimoto and K. Yano, *J. Catal.*, 2007, **251**, 249; (*e*) Y. Xiong, F. Wang, X. Huang, Y. Wen and X. Feng, *Chem.–Eur. J.*, 2007, **13**, 829.

11 A. Das, R. I. Kureshy, K. J. Prathap, M. K. Choudhary, G. V. S. Rao, N. H. Khan, S. H. R. Abdi and H. C. Bajaj, *Appl. Catal., A*, 2013, **459**, 97.

12 (*a*) R. I. Kureshy, K. J. Prathap, S. Agrawal, N. H. Khan, S. H. R. Abdi and R. V. Jasra, *Eur. J. Org. Chem.*, 2008, 3118; (*b*) M. Kumar, R. I. Kureshy, D. Ghosh, N. H. Khan, S. H. R. Abdi and H. C. Bajaj, *ChemCatChem*, 2013, **5**, 1; (*c*) R. I. Kureshy, K. J. Prathap, P. K. Bera, N. H. Khan, S. H. R. Abdi and H. C. Bajaj, *Tetrahedron*, 2011, **67**, 8300.

13 S. Patra and P. Paul, *Dalton Trans.*, 2009, 8683.

14 (*a*) J. Crassous, *Chem. Commun.*, 2012, **48**, 9684; (*b*) E. B. Bauer, *Chem. Soc. Rev.*, 2012, **41**, 3153; (*c*) P. Mosae Selvakumar, E. Suresh and P. S. Subramanian, *Polyhedron*, 2009, **28**, 245; (*d*) L.-S. Long, J.-W. Cai, Y.-P. Ren, Y.-X. Tong, X.-M. Chen, L.-N. Ji, R.-B. Huang and L.-S. Zheng, *J. Chem. Soc., Dalton Trans.*, 2001, 845; (*e*) S. Khatua, T. Harada, R. Kuroda and M. Battacharjee, *Chem. Commun.*, 2007, 3927; (*f*) H. Miyasaka, S. Okamura, T. Nakashima and N. Matsumoto, *Inorg. Chem.*, 1997, **36**, 4329; (*g*) U. Knof and A. V. Zelewsky, *Angew. Chem., Int. Ed.*, 1999, **38**, 302.

15 D. F. Evans, *J. Chem. Soc.*, 2003, 1959.

16 P. S. Subramanian, E. Suresh and R. S. Shukla, *Inorg. Chim. Acta*, 2005, **358**, 2651.

 This journal is © The Royal Society of Chemistry 2014